Revista Chilena de Historia Natural
78: 469-488, 2005

20th century fluctuations in the abundance of siliceous microorganisms preserved in the sediments of the Puyuhuapi Channel (44° S), Chile

Fluctuaciones en la abundancia de microorganismos silíceos preservados en los sedimentos del canal Puyuhuapi (44° S), Chile, durante el siglo XX

LORENA REBOLLEDO[1, 2, 3 *], CARINA B. LANGE[2, 3], DANTE FIGUEROA[4], SILVIO PANTOJA[2, 3], PRÁXEDES MUÑOZ[2, 5] & RODRIGO CASTRO[2]

[1]Programa de Postgrado en Oceanografía, Departamento de Oceanografía, Facultad de Ciencias Naturales y Oceanográficas, [2]Centro de Investigación Oceanográfica en el Pacífico Sur-Oriental (FONDAP-COPAS), [3]Departamento de Oceanografía, Facultad de Ciencias Naturales y Oceanográficas, [4] Departamento de Geofísica (DGF), Facultad de Ciencias Físicas y Matemáticas, Universidad de Concepción, Casilla 160-C, Barrio Universitario, Concepción Chile
[5]Universidad Católica del Norte, Casilla 117, Coquimbo, Chile
*Corresponding author: e-mail: lrebolle@udec.cl

ABSTRACT

We present a 100-year reconstruction of siliceous export production from sediments of the Puyuhuapi Channel (44° S, 70° W) in the Chilean fjords. We use accumulation rates and concentrations of diatoms and silicoflagellates, organic carbon (C_{org}) and biogenic opal (Si_{OPAL}) as proxies of export production, and fluctuations in the contribution of freshwater diatoms as proxies of rainfall in the hinterland and river runoff. Box core sediments collected at two sites within the Puyuhuapi Channel were analyzed: Station 35 (at the head of the fjord; 56 m water depth) and Station 40 (in the middle of the Channel; 270 m water depth). Surface sedimentation rates were 0.75 cm yr^{-1} at Station 35 and 0.25 cm yr^{-1} at Station 40. Si_{OPAL} content averaged ~ 4 % at both sites. Diatom accumulation rates as well as the contribution of freshwater diatoms were higher at the head of the fjord (1.59 10^{10} valves m^{-2} yr^{-1} and 22 %, respectively) than in its middle (1.08 10^{10} valves m^{-2} yr^{-1} and 14 %, respectively). Diatom abundances were two orders of magnitude higher than silicoflagellate contribution at both sites. In general, diatoms typical of high nutrient environments characterize the Puyuhuapi Channel sediments: at both sites, spores of the genus *Chaetoceros* dominated the diatom assemblage (> 40 % of total diatoms; spores of *Chaetoceros radicans*/*cinctus*, *Ch. constrictus*/*vanheurcki*, *Ch. debilis* and *Ch. diadema*). Downcore analysis reveals an overall increase in the production of siliceous microorganisms from the late 19th century to the early 1980s, and then a decrease until the late-1990s. We associate a decrease in freshwater diatom contribution since the mid-1970s which we associate with a concomitant decline in rainfall in the Chilean fjords. We suggest that this decline is related to the global atmospheric and oceanic warming of the past ~ 25 years.

Key words: siliceous microorganisms, diatoms, sediments, export production, Puyuhuapi Channel, Chilean fjords.

RESUMEN

Se presenta una reconstrucción de 100 años de la productividad silícea exportada en sedimentos del canal Puyuhuapi (44° S, 70° O) en los fiordos chilenos. Se utilizan las tasas de acumulación y las concentraciones de diatomeas y silicoflagelados, carbono orgánico (C_{org}) y sílice biogénico (Si_{OPAL}) como indicadores de la producción exportada y las fluctuaciones en la contribución de diatomeas de agua dulce como indicadores de precipitación y descargas de ríos. Se analizaron muestras de sedimentos colectadas mediante un sacatestigo de caja en dos sitios en el canal Puyuhuapi: Estación 35 (ubicada en la cabeza del fiordo dentro del seno Ventisquero; 56 m de profundidad) y Estación 40 (en la mitad del canal; 270 m de profundidad de agua). Las tasas de sedimentación superficial fueron de 0,75 cm $año^{-1}$ en la Estación 35 y 0,25 cm $año^{-1}$ en la Estación 40. En ambos sitios el contenido promedio de Si_{OPAL} fue de ~ 4 %. Las tasas de acumulación de diatomeas así como la contribución de diatomeas de agua dulce fueron más altas en la cabeza del fiordo (1,59 10^{10} valvas m^{-2} $año^{-1}$ y 22 %) que en la mitad de este (1,08 10^{10} valvas m^{-2} $año^{-1}$ y 14 % respectivamente). Las abundancias de diatomeas fueron dos órdenes de magnitud más altas que la contribución de silicoflagelados. En general, los sedimentos del canal Puyuhuapi son caracterizados por diatomeas típicas de ambientes de altos nutrientes: en ambos sitios, las esporas del género *Chaetoceros* dominan la asociación de diatomeas (> 40 % de la asociación total de diatomeas, esporas de *Chaetoceros*

radicans/*cinctus*, *Ch. constrictus*/*vanheurcki*, *Ch. debilis* y *Ch. diadema*). En general se observa un aumento en la tasa de acumulación de microorganismos silíceos desde finales del siglo XIX hasta comienzos de 1980, y un descenso hacia finales de la década de 1990. Asociamos una disminución en la diatomeas, sílice biogénico y silicoflagelados hacia el presente, sugiriendo una reducción en la productividad. Esto es acompañado por una disminución en las diatomeas de agua dulce desde mediados de los años 1970, con una disminución concomitante en la precipitación en el área de los fiordos chilenos. Sugerimos que dicha disminución se relaciona con el calentamiento atmosférico y oceánico global de los últimos 25 años.

Palabras clave: microorganismos silíceos, diatomeas, sedimentos, producción exportada, canal Puyuhuapi, fiordos chilenos.

INTRODUCTION

The Chilean fjords, located between 41° and 56° S, extend for 1,600 km and cover an area of 241,000 km^2 with a large number of islands, basins, and gulfs, formed by glacial erosion during the Quaternary and tectonic sinking of the central Chilean valley (Borgel 1970). The fjords present three glacial systems: North Patagonian Icefield (46-47° S), South Patagonian Icefield (48-52° S) and Darwin Mountains Icefield in Tierra del Fuego (54-55° S), which together cover 19,000 km^2 (Warren & Aniya 1999). There are also several glaciers that descend along the costal line at the head of the fjords, creating icebergs that mix with salt water.

There has been little research on the Chilean fjords from a paleoclimatic and paleoceanographic point of view, in spite of the fact that the fjords present high sedimentation rates, a large quantity of terrestrial sediments contributed by river discharge, and an adequate preservation of marine and continental proxies that provide a unique opportunity to study the paleoenvironmental history with high temporal resolution. At present, there are strong latitudinal gradients in surface ocean temperature and salinity (Levitus & Boyer 1994) that suggest that this region has also been sensitive to changes in the past.

Presently, the fjords, channels and gulfs of southern Chile are influenced by three water masses between 0 and 600 m (e.g., Silva et al. 1998a): (a) Subantarctic Surface Water between 0 and 150 m, which mixes with freshwater during its introduction into the channels being modified into Subantarctic Surface Modified Water (Silva et al. 1995); (b) Equatorial Subsurface Water between 150 and 300 m until 48° S (Silva & Neshyba 1979); and (c) Antarctic Intermediate Water below depths of 300 m.

Some chemical aspects of the Chilean fjord sediments have been studied by Ahumada et al. (1996), Silva et al. (1997), Silva et al. (1998b), Pantoja et al. (2002), Rojas (2002), Silva & Prego (2002), Sepúlveda et al. (in press), among others. Geochronology studies have been performed by Salamanca (1996), using ^{210}Pb, who registered sedimentation rates of 0.19-0.41 cm year^{-1} between 45-46º S, by Leventer et al. (1995)[1] who reported values of 0.03-0.165 cm year^{-1} between 42-54° S, and by Anderson & Archer (1999) who dated cores from the western region of the Magellan Strait, using ^{14}C, and recording sedimentation rates of 13-27 cm 1.000 years^{-1}.

The oceanic zone off Chiloé exhibits a high productivity that apparently has increased during the Holocene. Lamy et al. (2002) propose that this increment is strongly tied to the nutrient supply from the Southern Ocean by the Antarctic Circumpolar Current (ACC) and relate it to a northward displacement of the ACC and the Southern Westerlies by 5º latitude from its present position. At present, the Southern Westerlies, together with the morphology of the Andes barrier, cause a precipitation gradient in Chile producing typical cold temperate climate conditions without a seasonal signal south of 43°S (Devynck 1971). Consequently, the Chilean fjord zone presents precipitations between 1,000 and 7,000 mm year^{-1} (DGA 1987), and maximum mean annual river discharge of 2,470, 3,480 and 3,340 m^3 s^{-1} at 42, 46 and 50° S, respectively (Dávila et al. 2002).

To date, there is only one scientific work (Sepúlveda et al. accepted) that reports on the productivity fluctuations of the Chilean fjords

[1] LEVENTER A, S ISHMAN, J STRAVERS, S AAVANG (1995) Holocene sedimentation rates on the southern Chilean continental margin. Abstract O52B. AGU Spring Meeting, 1995. S185

throughout the last century. These authors analyzed various productivity proxies in the sediments (especially organic carbon, pigments, amino acids and biogenic silica) and indicate a constant increase in productivity from the late 19th century to the early 1980s, a decrease until the late-1990s, and a rise thereafter to present-day values.

The main objective of this work is to detail the variations in siliceous export production during the last ~100 years using the biogenic silica content and the abundance and composition of siliceous microorganisms (diatoms and silicoflagellates) preserved in the sediments of the Puyuhuapi Channel (~44° S). This new database allows us to (a) correlate the biogenic silica content with diatoms and silicoflagellates, (b) infer changes in the specific composition of these siliceous microorganisms, and (c) associate the temporal fluctuations of freshwater diatom contribution with the historical variations in rainfall in the study area.

Study area

The Puyuhuapi Channel is approximately 60 miles long with its main axis oriented in a SW-NE direction. To the northeast, the Puyuhuapi Channel is connected with the Jacaf Channel; in the south, it connects with the Moraleda Channel (Fig. 1). Its northernmost part, the Ventisquero Sound, is separated into two sectors (north and south) by the Galvarino Pass (Valle-Levinson et al. 2001). The depth varies from 40 m in the northern sector, to 10 m at the shallowest part of the sill and to 80 m in the southern part.

There is no information on circulation in the Puyuhuapi Channel except for two studies (Valle-Levinson et al. 2001, Cáceres & Valle-Levinson 2004) that concentrated on the flow on both sides of Galvarine Pass. The latter described an anticlokwise flow throughout the water column in the northern side of the pass and suggested sluggish flushing and longer residences times of the water in the northern basin than in the south. In adition, the shallowest and narrowest section within the pass seems to represent a boundary between inflows and outflows (Cáceres & Valle-Levinson 2004).

The Puyuhuapi Channel is poor in dissolved oxygen with values < 2.5 mL L^{-1} at depths below 150 m (Silva et al. 1997). Primary productivity was measured within the channel during the Cimar Fiordos 7 spring cruise, yielding values of 47.8 mg C m^{-2} h^{-1} at the head and 6.6 mg C m^{-2} h^{-1} at the mouth of the fjord (integrated values to 25 m water column depth) (Astoreca et al. 2002). In general, the distribution of the nutrients in the water column has been described as having a two layer structure, with very low concentrations in the surface waters, a strong nutricline at about 10-20 m depth and higher values at depth (Silva et al. 1997). The sediments are composed of silt and clay and are relatively rich in organic matter (10 %), with average values of total organic carbon (1.62 %) and total nitrogen (0.17 %) (Silva & Prego 2002).

The Ventisquero and Cisnes rivers, with a drainage area of 272 and 5,163 km^2 respectively, discharge into the Ventisquero Sound (the former) and the Puyuhuapi Channel (the latter). The Ventisquero River has an average flow of 35 m^3 s^{-1} (average for 1995-2000), while the existing data for the Cisnes River (limited to four months of 2001) indicates a water flow of 183 m^3 s^{-1}. Due to these fresh water inputs a well defined pycnocline has been described (Silva et al. 1995, 1997).

MATERIAL AND METHODS

The sediments analyzed in this study come from the Ventisquero Sound (station 35: 44°21.37' S, 72°34.82' W; 56 m water column depth) and from the middle of the Puyuhuapi Channel (station 40: 44°49.39' S, 72°56.02' W; 270 m), and were collected on board the AGOR "Vidal Gormaz" vessel of the Chilean Navy during the Cimar Fiordos 7 oceanographic cruise of November 2001 (Fig. 1).

A box corer was used to collect the sediments; each box core cast was sub-sampled on board using 7-cm diameter PVC tubes. The tubes were sectioned in 1-cm intervals and the samples stored in plastic bags and frozen at -20° C for later analysis in the laboratory. The cores used in this study were 32 cm (station 35) and 25 cm long (station 40).

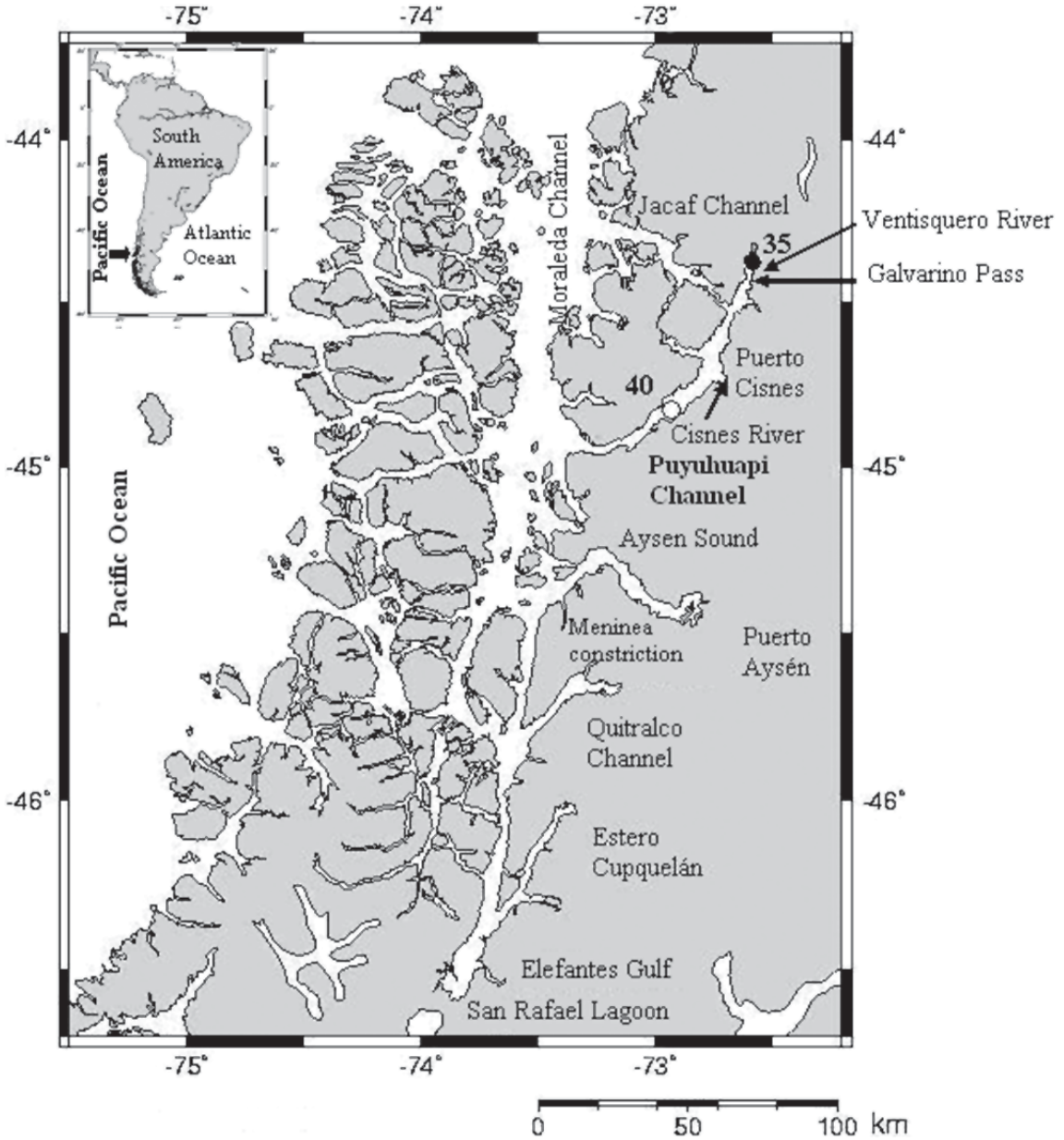

Fig. 1: Location of cores collected in the Puyuhuapi Channel: station 35 (44°21.37' S; 72°34.82' W) and 40 (44°49.39' S; 72°56.02' W).

Ubicación de los testigos recolectados en el canal Puyuhuapi: estación 35 (44°21,37' S; 72°34,70' O) y 40 (44°49,39' S, 72°56,02' O).

Organic carbon (C_{org}) determinations were made with an elemental analyzer Tekmar Dorman. The lyophilized samples were previously ground and transferred to glass vials and acidified with HCl 15% (until effervescence). The remaining acid was evaporated at 80 ºC for 2.

In each sample, the biogenic silica content was determined following the molybdenum blue method of Mortlock & Froelich (1989). This method has two steps: the first one consists in the extraction of silica from the lyophilized sediment matrix, and the second step is the determination of the absorbance of the solution at 812 nm. The values reported here are expressed as: $\% Si_{OPAL} = 112.4*(Cs/M)$ where Cs = silica concentration in the sample

in (mM), M = sample mass in mg, and 112.4 = molecular weight of Si (28.09) * the extraction volumen of NaOH (0.04 L) *100; and as Si_{OPAL} accumulation rate (g m^{-2} yr^{-1}) derived from the constant rate of supply (CRS) model of ^{210}Pb deposition (see below).

For the study of the siliceous microorganisms, the station 40 core was analyzed in its totality while some sediment intervals were selected for the station 35 core. Wet sediment samples were dried and ~1.5 g of dry sediment was treated aacording to the technique described in Schrader & Gersonde (1978) with some modifications. The dry sediment was mixed into a solution of sodium pyrophosphate, hydrogen peroxide 25 %, and distilled water; this was heated and boiled for 30 minutes; hydrochloric acid was added, and boiled once again and then left to settle for 12 hours. Subsequently, it was repeatedly rinsed with distilled water until reaching a neutral pH. Permanent slides of acid-cleaned material were prepared by placing a defined sample volume (0.2 mL) onto a microscope slide, air-dried and mounted with Naphrax mounting medium. Two permanent slides per sample were prepared in this fashion.

Qualitative and quantitative analyses of diatoms and silicoflagellates were performed at X 400 and X 1000 using a Zeiss-Axioscope two plus microscope with phase-contrast illumination. For diatoms, several traverses across each cover slip were examined, depending on microorganism abundances. At least two cover slips per sample were examined in this way. About 300 valves were counted for each cover slip. For silicoflagellates, 1/5 of each cover slip was counted. Counting of replicate slides indicated that the analytical error of the concentration estimates is < 15 %. The counting procedure and definition of counting units for diatoms also followed those of Schrader & Gersonde (1978).

The total number of organisms per slide was calculated as $N = ni\ (A/a)$, where A = total area of the cover slip in (mm^2) $\pi * r^2$; a = area counted (mm^2), ni = number of individuals per counted area. The total abundance of each taxon and/or group of taxa was expressed as concentration per gram of dry sediment (C_{prof}):

$$C_{prof} = N\ (V/v)/\text{sample dry weight (g)}$$

where N = total number of diatoms or silicoflagellates in the slide, V = volume of diluted sample (200 mL), v = volume of aliquot placed onto slide (0.2 mL).

Diatoms were identified to the lowest taxonomic level possible, based principally on the works of: Cupp (1943), Rivera (1981), Round et al. (1990), Sims (1996), Thomas (1997), Jensen & Moestrup (1998) and Witkowski et al. (2000). For silicoflagellate species, Takahashi & Blackwelder (1992) was used.

The Shannon-Wiener diversity index (Brower et al. 1998) for each sample was calculated as $H' = -\sum pi\ log\ pi$, where pi = ni / N, pi = the proportion of the total number of individuals per species in each sample, ni = number of individuals per species, N = total number of individuals per sample.

Accumulation rates (Ac) of siliceous microorganisms and of Si_{OPAL} were calculated based on their respective concentrations in each 1-cm interval of the core (C_z), multiplied by the bulk density (r) and the sedimentation rate estimated from the age (t) at each core depth ($Ac = C_z * r * z/t$).

The age at each core depth was derived from radiometric dating using ^{210}Pb, as follows: $t_z = -t_{210} * ln(I_z/I_o)$, where τ^{210} is the decay constant of ^{210}Pb (32.18 yr), and Io and I_z are the unsupported ^{210}Pb inventories ($^{210}Pb_{xs}$) in the core (total) and below depth z, respectively. The inventories (I_0 and I_z) are estimated from $I = \sum A_i\ \rho_i\ h_i$ where A_i is the $^{210}Pb_{xs}$ (dpmg g^{-1}), ρ_i the bulk density in the i interval (g cm^{-3}) and h_i is the thickness of the i interval. The unsupported activities were estimated from total ^{210}Pb minus the asymptotic ^{210}Pb activity at depth, assumed to be in equilibrium with ^{226}Ra in the sediment (McCaffrey & Thomson 1980, Cochran et al. 1998).

The ^{210}Pb activities were determined by alpha spectrometry of its daughter, ^{210}Po (Flynn 1968), and the constant rate supply (CRS) model (Appleby & Oldfield 1978, Binford & Brenner 1986, McCaffrey & Thomson 1980, Cochran et al. 1998). This method has been extensively used in lakes and coastal sediments, and assumes (a) a constant input of $^{210}Pb_{xs}$ (unsupported) to the sediments, unaffected by changes in sediment type or sedimentation rate, and (b) that there has been no significant redistribution after deposition.These assumptions are reasonable for shallow, non bioturbated sediments.

Standardized anomalies of the precipitation and freshwater diatom records were calculated as: $X-\bar{X}/SD$, where $\bar{X}$ is the value of the respective parameter, X is the average of the entire record, and SD is the standard deviation.

RESULTS

The sediments were characterized by a dark olive color. A sand layer was present at 12-15 cm in core 40 which probably was the product of a turbidity flow, according to preliminary sediment observation. The samples between 22 and 25 cm contained a large quantity of leaf remains of continental origin. A sand layer was not observed in core 35, but leaf remains were seen in the deepest intervals.

Chronology

No evidence of biological activity (burrow structures, shells, living animals) was observed during sampling; only in core 35 did we observe a mixed layer in the upper 4 cm. Thus, the CRS model applied to these sediments seems to be a reasonable dating method. Based on the $^{210}Pb_{xs}$ inventories, the ages were considered reliable down to 6-7 cm and 25-26 cm for cores 40 and 35, respectively (Table 1). Below these depths ages are uncertain and extremely high due to exponential increment of the errors inherent to the dating method (Binford 1990). Assuming that the surface sediments represent the year 2001 (collection year), core 40 has an age of 38 years at 6 cm (AD 1963), and core 35 of 102 years (AD 1899) at 25 cm depth (Table 1).

TABLE 1

Bulk density data and ages in cores 35 and 40

Densidad aparente y edad de cada estrato de los testigos recolectados en las estaciones 35 y 40

	Station 35			Station 40		
Depth in core (cm)	Bulk density (g cm^{-3})	Interval (years)	Year (AD)	Bulk density (g cm^{-3})	Interval (years)	Year (AD)
0	0.30	0	2001	0.43	0	2001
1	0.31	1.52	1999	0.45	4.21	1997
2	0.38	1.54	1998	0.48	3.75	1993
3	0.49	1.89	1996	0.51	5.67	1987
4	0.50	2.20	1994	0.63	6.98	1980
5	0.52	2.51	1991	0.51	9.03	1971
6	0.54	2.66	1989	0.59	8.02	1963
7	0.55	2.80	1986			
8	0.53	2.78	1983			
9	0.55	2.61	1980			
10	0.56	2.83	1978			
11	0.59	3.03	1975			
12	0.57	3.38	1971			
13	0.55	3.50	1968			
14	0.61	3.72	1964			
15	0.64	3.59	1960			
16	0.61	3.85	1957			
17	0.66	3.97	1953			
18	0.64	3.99	1949			
19	0.68	5.22	1943			
20	0.63	4.81	1939			
21	0.66	5.69	1933			
22	0.67	6.04	1927			
23	0.62	7.53	1919			
24	0.62	9.46	1910			
25	0.68	11.34	1899			

Organic carbon content, % Si_{OPAL}, diatom and silicoflagellate concentration and accumulation

Organic carbon (C_{org}; Fig. 2A, 2C) at station 35 varied between 0.7 (29-30 cm) and 1.8 % (0-1 cm) ($\bar{X}$ = 1.3 %), and between 0.3 (sand layer) and 7.6 % (leaf remains) (X = 2.2 %) in station 40. The average Si_{OPAL} content was similar at both sites ($\bar{X}$ = ~ 4 %), but the pattern was different. At station 35, the Si_{OPAL} values showed an abrupt jump at 7 cm depth, from ~4 % to ~6 %; above 7 cm, the average was 3.8 %, while below 7 cm it was 4.9 % (Fig. 2A). In contrast, the Si_{OPAL} record of station 40 was strongly affected by the presence of the sand layer and the leaf remains, presenting large fluctuations in Si_{OPAL} values (1-6 %) (Fig. 2C).

Microscope analysis revealed the dominance of diatoms in the sediments, followed by silicoflagellates; radiolarians, Chrysophyta cysts and sponge spicules were rare. The diatom concentration in the surface sediment of station 35 was moderately greater ($1.9\ 10^7$ valves g^{-1}, Fig. 2B) than at station 40 ($9.9\ 10^6$ valves g^{-1}, Fig. 2D), but at both sites diatom concentrations were two orders of magnitude greater than that of silicoflagellates (10^5 skeletons g^{-1}; Fig. 2B and 2D). Both microorganisms were scarce in the sand layer and in the deeper interval consisting of leaf remains (station 40). The correlation between diatoms and silicoflagellates was positive and significant: Station 40: $r^2 = 0.64$, n = 22, $P < 0.001$; station 35: $r^2 = 0.52$, n = 12, $P < 0.01$.

Diatom accumulation rates fluctuated around 10^{10} valves m^{-2} $year^{-1}$ at both stations, while accumulation rates for silicoflagellates were $2\ 10^8$ skeletons m^{-2} $year^{-1}$ at station 35 and $9\ 10^7$ skeleton m^{-2} $year^{-1}$ at station 40 (Fig. 3A, 3B). Si_{OPAL} accumulation rates were almost twice as high at station 35 than at station 40. Diatoms seem to modulate Si_{OPAL} fluctuations; the regression index r^2 between diatom accumulations (log-transformed data) and those of Si_{OPAL} presented values of 0.46 (station 35) and 0.84 (station 40), while the correlation between silicoflagellates and Si_{OPAL} was much lower ($r^2 = 0.34$, $P < 0.05$ and 0.11, $P = 0.52$, respectively).

It is interesting to note that the accumulation rates of diatoms, silicoflagellates and Si_{OPAL} at station 35 increase from the end of the 19th century to the beginning of the 1980s (Fig. 3A); starting at that time the pattern changes: Si_{OPAL} accumulation rates decrease toward the present while the rates of the siliceous microorganisms continue to increase but include an abrupt drop in 1998-1999. The short record of station 40 also shows an increase in accumulation rates over time, and a decoupling of the silicoflagellates with Si_{OPAL} and diatoms beginning in the late 1980s (Fig. 3B).

Diatoms and silicoflagellates

A total of 98 taxa of diatoms and three species of silicoflagellates were found in the two cores. At station 35, the diversity index (H') varied between 2.5 (2-3 cm) and 3.9 (7-8 cm) with an average value of H' = 3.0 (typical for a coastal environment, Margalef 1978). The dominant diatom assemblage was represented by *Chaetoceros* spp. (26 %), *Rhizosolenia setigera/pungens* (13 %) and *Cyclotella* sp. (11 %) followed by *Skeletonema costatum*, *Chaetoceros muelleri* spores, *Rhizosolenia* sp. 1, *Thalassionema nitzschioides* var. *nitzschioides* and *Paralia sulcata*, among others (Table 2; Fig. 4). Diversity was homogenous at station 40 with an average value of H' = 2.4. *Chaetoceros* spp. spores (~50 % of the total) dominated the assemblage, accompanied by *Skeletonema costatum*, *Cyclotella* spp., *Thalassionema nitzschioides*, *Rhizosolenia setigera/pungens*, and several species of small-sized *Thalassiosira*, in decreasing order of importance (Table 2; Fig. 4).

Three silicoflagellates species were recorded at both sites: *Distephanus speculum*, *Dictyocha messanensis messanensis* and *D. mandrai*. *D. speculum* was the dominant species contributing over 90 % to the silicoflagellate assemblage (Table 2; Fig. 4).

Ecological groups

All diatom species or groups of species, found in at least one sample, were assigned to each of the following six ecological cathegories (Appendix 1): high nutrients (HN), coastal planktonic (CP), marine benthic (MB), cold water (CW), warm water (WW) and freshwater (FW). The grouping is based on ecological characteristics as stated in well-known bibliographies on the distribution of extant diatoms (Cupp 1943, Round et al. 1990, Sims 1996, Witkowski et al. 2000, Romero &

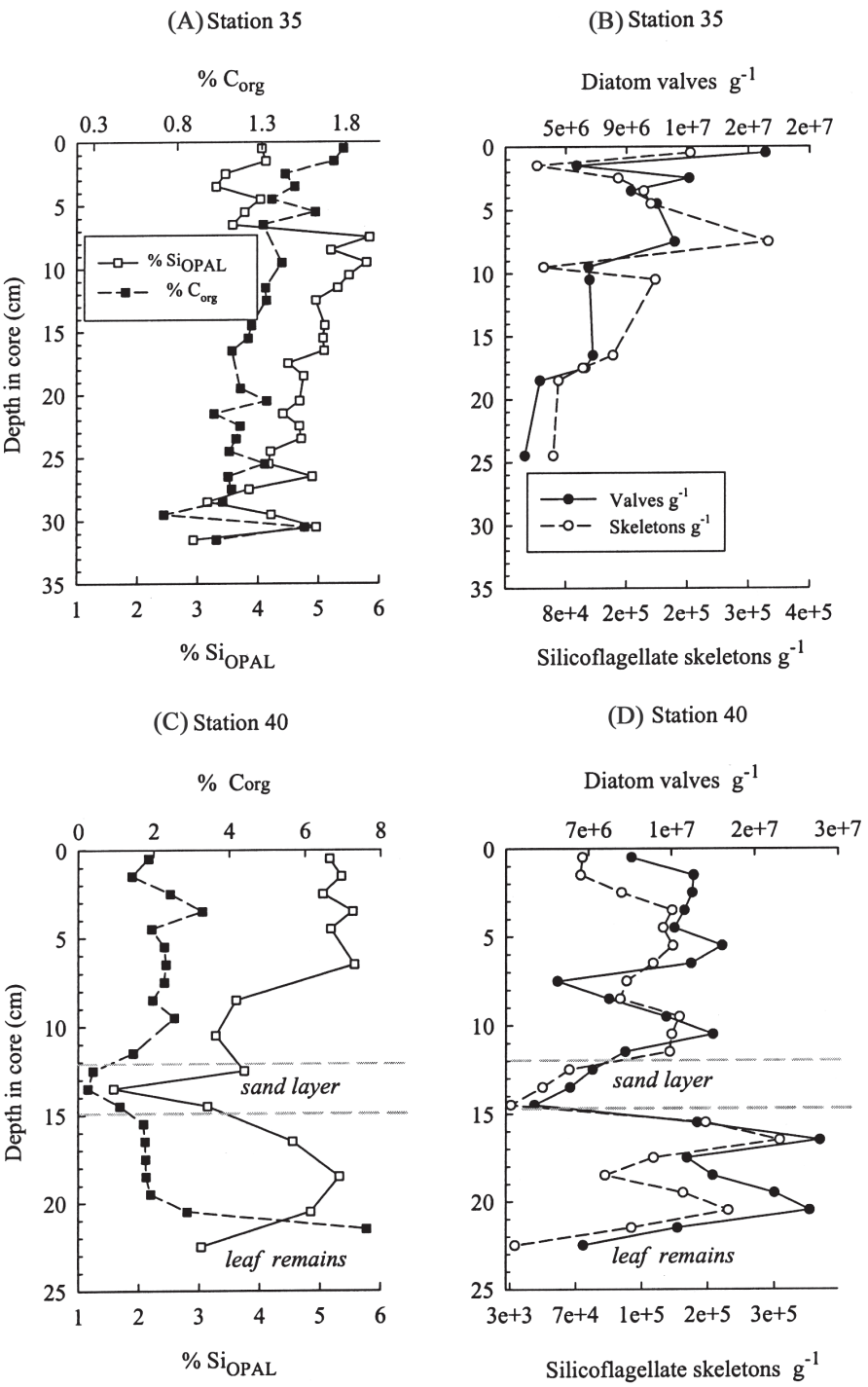

Fig. 2: Downcore profiles stations 35 (A, B) and 40 (C, D); (A) and (C): relative contribution (%) organic carbon (C_{org}, black squares) and biogenic silica (Si_{OPAL}, white squares); (B) and (D): concentration of diatoms (black circles) and silicoflagellates (white circles) in valves and skeletons g^{-1}, respectively. The presence of the sand layer between 12 and 15 cm, and the terrestrial leaf detritus layer is indicated in core 40.

Perfiles estaciones 35 (A, B) y 40 (C, D); (A) y (C): contribución relativa (%) de carbono orgánico (C_{org}, cuadrados negros) y de sílice biogénica (Si_{OPAL}, cuadrados blancos). (B) y (D): concentración de diatomeas (círculos negros) y silicoflagelados (círculos blancos) en valvas y esqueletos g^{-1}, respectivamente. En el testigo 40 se señala la presencia de la capa de arena entre los 12- 15 cm y el horizonte con detritos terrestres de hojas.

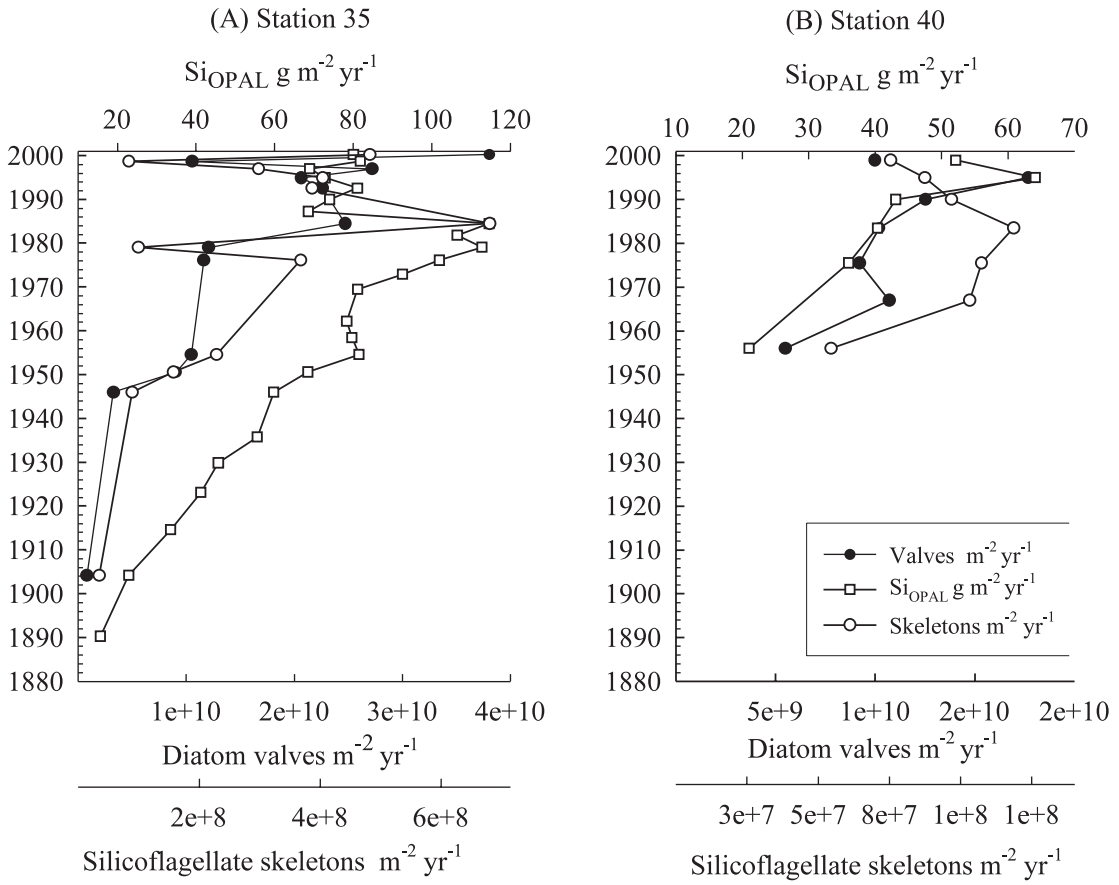

Fig. 3: Accumulation of diatoms (valves m^{-2} year^{-1}; black circles), silicoflagellates (skeletons m^{-2} yr^{-1}; white circles) and Si$_{OPAL}$ (g m^{-2} year^{-1}; white squares) at stations 35 (A) and 40 (B).

Acumulación de diatomeas (valvas m^{-2} año^{-1}; círculos negros), silicoflagelados (esqueletos m^{-2} año^{-1}; círculos blancos) y Si$_{OPAL}$ (g m^{-2} año^{-1}; cuadrados blancos) en las estaciones 35 (A) y 40 (B).

Hebbeln 2003). Sediments at station 35 were characterized by the high nutrients group (dominated by *Chaetoceros radicans*/*cinctus* and *Ch. constrictus*/*vanheurcki* spores) with an average contribution of 36 % (Fig. 5) and a strong presence of freshwater diatoms (21 %, e.g., *Cyclotella* spp., *Chaetoceros muelleri*). These two groups were accompanied by coastal planktonic (28 %; e.g., *Rhizosolenia setigera*/*pungens*) and marine benthic species (9 %; e.g., *Opephora pacifica, Paralia sulcata, Diploneis* spp.) (Fig. 5). The contribution of the high nutrient group at station 40 was much greater than at station 35, comprising, on average, 60 % of the total diatom assemblage (Fig. 5). This group was accompanied by coastal planktonic (15 %), freshwater (13 %) and marine benthic diatoms (5 %). The cold-water group at both stations did not exceed 6 %, and showed a slight tendency toward higher values in the deeper intervals. The warm water group was very poorly represented. At station 35, this group was absent throughout the core except at 25 cm core depth, while it reached 4 % in the 4-5 cm interval at station 40 (Fig. 5).

The classification of silicoflagellates into water mass affinity groups was based on the work of Takahashi & Blackwelder (1992) who characterized *D. speculum* as typical of cold waters, *D. mandrai* of temperate-cold waters, and *D. messanensis messanensis* of warm waters. *D. speculum* comprised more than 90 % of the silicoflagellate assemblage in both cores (Fig. 6). The contribution of *D. messanensis messanensis* (4-9 %) was noteworthy in the interval 6-13 cm at station 40 and in the interval 17-18 cm of station 35, while the record of *D. mandrai* was sporadic (Fig. 6).

TABLE 2

Diatoms and silicoflagellates that characterize the sediments of the Puyuhuapi Channel. The species are presented in decreasing order according to their average contribution to the total assemblage (%). Shaded areas indicate taxa with relative percentage > 1%

Diatomeas y silicoflagelados que caracterizan los sedimentos del canal Puyuhuapi. Las especies fueron ordenadas en forma decreciente de acuerdo a su promedio de contribución a la asociación total (%). Las áreas sombreadas indican aquellos taxa cuyo porcentaje relativo es > 1%

Diatom	Percentage station 35	Percentage station 40
Chaetoceros spp. (spores)	26.5	47.3
Rhizosolenia setigera/pungens	13.0	3.8
Cyclotella spp.	11.3	8.4
Skeletonema costatum	5.7	8.5
Chaetoceros muelleri (spores)	3.9	0.9
Rhizosolenia sp. 1	3.7	0.9
Thalassionema nitzschioides var. *nitzschioides*	3.5	4.1
Paralia sulcata	2.5	0.6
Pennate diatom sp.	2.3	2.3
Thalassiosira eccentrica	2.1	1.6
Thalassiosira spp. (5-12 μm)	2.0	2.4
Opephora pacifica	1.9	1.0
Thalassiosira sp. 1	1.8	0.5
Diploneis spp.	1.3	0.2
Thalassiosira tenera	1.3	0.5
Melosira spp.	1.1	0.3
Thalassiosira gerloffii	1.0	1.9
Achnanthes spp.	0.9	1.4
Ditylum brightwellii	0.8	1.5
Centric diatom sp.	0.8	1.6
Cocconeis spp.	0.7	1.4
Thalassiosira pacifica	0.4	1.6
Silicoflagellates		
Distephanus speculum	98.5	92.2
Dictyocha messanensis messanensis	1.4	4.8
Dictyocha mandrai	0.1	3.0

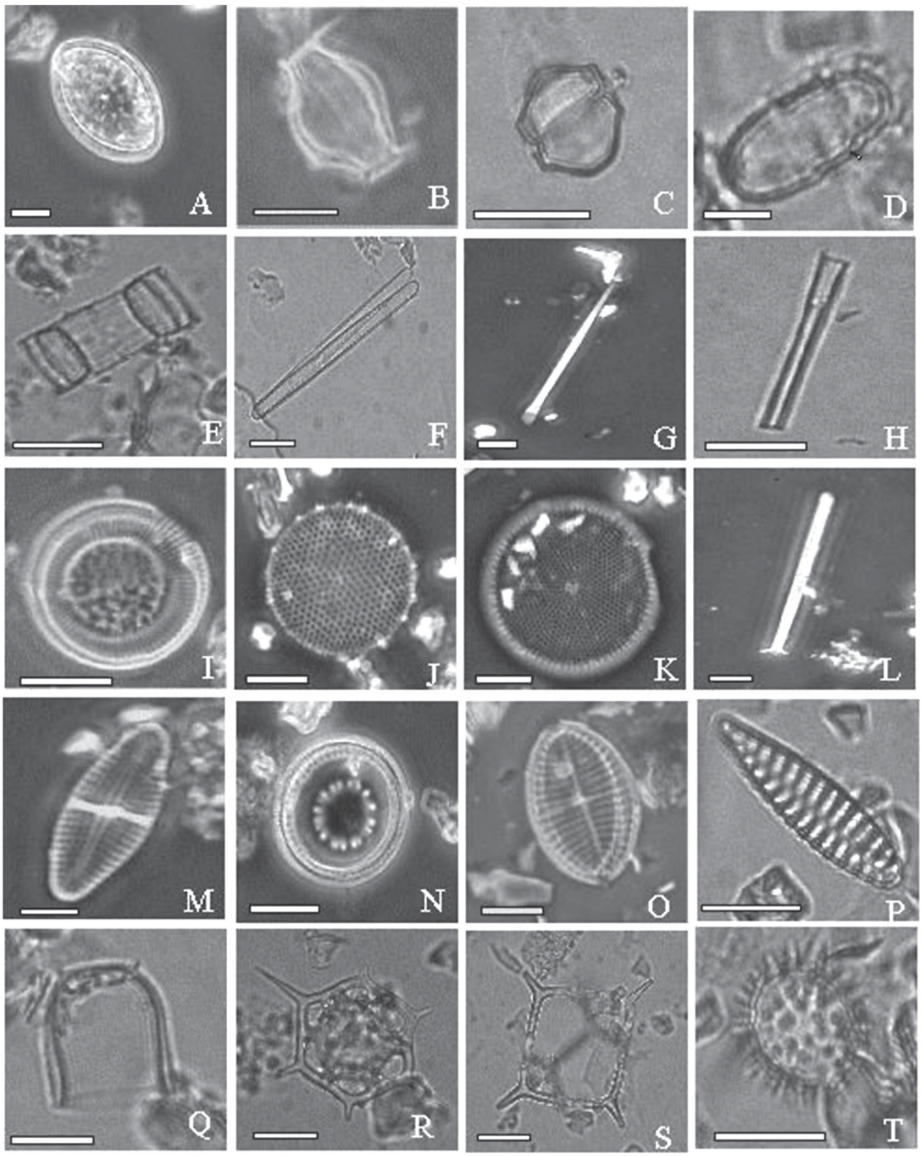

Fig. 4: Main taxa of siliceous microorganisms present in Puyuhuapi Channel sediments. Fig. (A)-(Q): diatoms. Fig. (R)-(S): silicoflagellates. Fig. (T): chrysophyte cyst. (A) Valve view of resting spore of *Chaetoceros constrictus*/*vanheurcki*. (B) Girdle view of resting spore of *Chaetoceros* sp. (C) Girdle view of *Chaetoceros radicans*. (D) Girdle view of resting spore of *Chaetoceros muelleri*. (E) *Skeletonema costatum*. (F) *Thalassionema nitzschioides* var. *nitzschioides*. (G) Process of *Rhizosolenia pungens*. (H) Process of *Rhizosolenia* sp. 1. (I) Valve view *Cyclotella litoralis*. (J) *Thalassiosira eccentrica*. (K) *Thalassiosira gerloffii*. (L) Process of *Ditylum brightwellii*. (M) *Achnanthes* sp. (N) *Paralia sulcata*. (O) *Cocconeis* sp. (P) *Opephora pacifica*. (Q) *Melosira arctica*. (R). *Distephanus speculum*. (S) *Dictyocha messanensis messanensis*. (T) Crysophyte cyst. Scale = 10 μm in figs (A)-(C), (E)-(P), (R)-(S). Scale = 5 μm in figs (D), (Q) and (T).

Principales taxa de microorganismos silíceos presentes en los sedimentos del canal Puyuhuapi. Fig. (A)-(Q): diatomeas. Fig. (R)-(S): silicoflagelados. Fig. (T): quiste de Chrysophyta. (A). Vista valvar espora de *Chaetoceros constricuts*/*vanheurcki*. (B). Vista singular espora de *Chaetoceros* sp. (C). Vista singular espora de *Chaetoceros radicans*. (D). Vista singular espora de *Chaetoceros muelleri*. (E). *Skeletonema costatum*. (F). *Thalassionema nitzschioides* var. *nitzschioides* (G). Proceso de *Rhizosolenia pungens*. (H) Proceso de *Rhizosolenia* sp. 1. (I). Vista valvar *Cyclotella litoralis*. (J). *Thalassiosira eccentrica*. (K). *Thalassiosira gerloffii*. (L). Proceso de *Ditylum brightwellii*. (M). *Achnanthes* sp. (N) *Paralia sulcata*. (O) *Cocconeis* sp. (P) *Opephora pacifica*. (Q). *Melosira arctica*. (R). *Distephanus speculum*. (S). *Dictyocha messanensis messanensis*. (T). Quiste de Crysophyta. Escala = 10 μm en Figs. (A)-(C), (E)-(P), (R)-(S). Escala = 5 μm en Figs. (D), (Q) y (T).

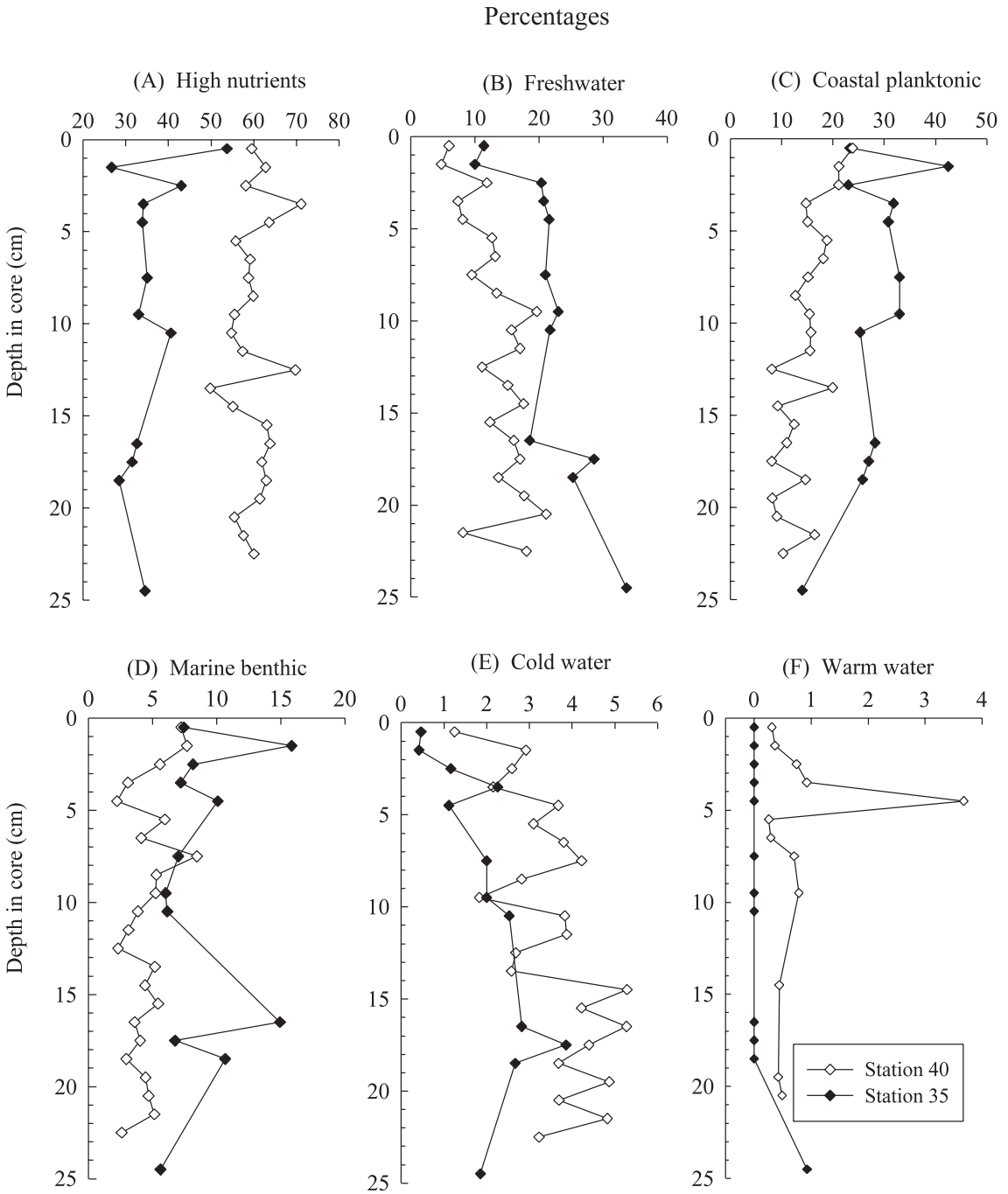

Fig. 5: Downcore profiles of the relative abundance (expressed as percentages of the whole diatom assemblage) of the six diatom ecological groups present in the Puyuhuapi Channel sediments, stations 35 (black circles) and (white 40 circles).

Perfiles de la variabilidad en la abundancia relativa (expresada como porcentaje del total de diatomeas) de los seis grupos ecológicos de diatomeas presentes en los sedimentos del canal Puyuhuapi, estaciones 35 (círculos negros) y 40 (círculos blancos).

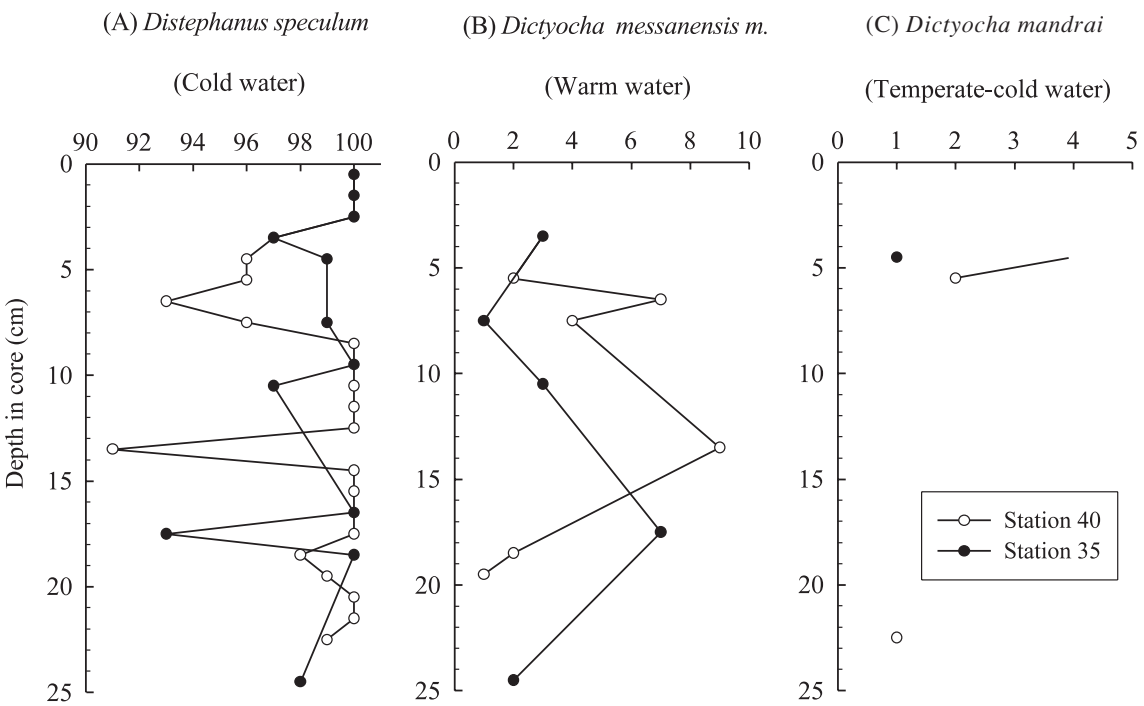

Fig. 6: Downcore profiles of the relative abundance (expressed as percentages of the whole silicoflagellate assemblage) of silicoflagellate species present in the sediments of the Puyuhuapi Channel, stations 35 (black circles) and (white 40 circles).

Perfiles de la variabilidad en la abundancia relativa (expresada como porcentaje del total de silicoflagelados) de las especies de silicoflagelados presentes en los sedimentos del canal Puyuhuapi, estaciones 35 (círculos negros) y 40 (círculos blancos).

Precipitation record

We collected precipitation data for two sites located adjacent to the study area: Puerto Cisnes (44°45' S-72º42' W), a port in the Puyuhuapi Channel, and Puerto Aysén (45°24' S-72°42' W) at the head of the Aysen Sound (Fig. 1). Precipitation at both stations follows a seasonal behavior with higher values between April and September. Available data[2] encompass the periods 1955-2002 for Puerto Cisnes and 1931-1999 for Puerto Aysén. In both records, rainfall values decrease from ~ 4000 mm yr^{-1} in AD 1958 to 2000 (Aysén) and 3000 mm yr^{-1} (Cisnes) in AD 1999-2001. The record is less variable for the older period (1931-1958) and values oscillate around 2,800 mm yr^{-1}.

[2] See Dirección General de Aguas (http:// www.dga.cl)

DISCUSSION

The Puyuhuapi Channel is characterized by high sedimentation rates (0.25-0.74 cm $year^{-1}$), similar to those registered for the Aysén Sound (0.19 cm $year^{-1}$) and the Costa Channel (0.28 cm $year^{-1}$) by Rojas (2002), and for Chacabuco Port (0.22 cm $year^{-1}$) by Salamanca (1996). The C_{org} was on average >1 % (with values ranging 0.7-3.3 %, except for the sections that contain the sand layer and the leaf remains), agreeing with the results recorded by Silva et al. (1997, 1998b) and Silva & Prego (2002) for the northern fjord zone between Puerto Montt and the Moraleda Channel.

Concentrations and accumulation rates of the productivity proxies (C_{org}, Si_{OPAL}, marine and freshwater diatoms, and silicoflagellates) were always greater at station 35 (Ventisquero Sound) than at station 40 (located in the middle of the

fjord) (Figs 2, 3). Higher values at St. 35 versus St 40 could be linked to (a) the fact that the Ventisquero Sound represents a shallower (56 versus 270 m at station 40; Araya 1997), more stable environmental depository, which is in agreement with the slow water flow observed by Cáceres & Valle-Levinson (2004; see "Study Area"); and/or (b) higher sedimentation rates and preservation of organic matter due to lower dissolved bottom oxygen concentrations (<1.5 mL L^{-1} at the head versus 3 mL L^{-1} at the mouth of the fjord, Silva et al. 1997).

Sepúlveda et al. (in press) sustain that the temporal fluctuations of these productivity proxies preserved in the sedimentary record reflect changes in (a) phytoplankton production and composition, (b) precipitation and river discharge, and (c) anthropogenic influence, which is most notable since the 1980s with the establishment of salmon farms. These authors define two contrasting periods in the Puyuhuapi Channel, 1890-1980 and 1980-2001. The former is characterized by high productivity, high correlation among proxies, and no significant correlation with rainfall anmalies. The latter, on the other hand, was described as period of decreased productivity and a significant correlation between freshwater diatom accumulation and the precipitation anomaly ($r^2 = 0.76$, $P < 0.05$).

Comparison with other siliceous microorganism studies in the area

There are no previous studies on siliceous microorganisms in the Chilean fjord sediments. The closest one to our study area is the work of Romero & Hebbeln (2003) who analyzed surface sediments of the continental margin off Chile, including the oceanic area off Chiloé (< 100 km off the coast) between 41 and 44° S. The values reported here on biogenic silica content (Si_{OPAL} 4-5 %) and diatoms (~10^7 valves g^{-1}) in the surface sediments of the Puyuhuapi Channel are higher than the values reported by Romero & Hebbeln (2003, 3.7 % and ~10^6 valves g^{-1}, respectively). Moreover, the relative contribution of the dominant diatom group in the Puyuhuapi Channel sediments which was represented by the "high nutrients group" (50-60 % of the total of diatoms), is much greater than the one reported by Romero & Hebbeln (2003) (13-37 %). As expected, the importance of freshwater diatoms (10 % versus ≤ 1%) was also greater in the Puyuhuapi Channel than in the oceanic zone. The differences between both areas (inside the fjords versus oceanic zone of Chiloé) are clearly highlighted in the satellite images (see images in Acha et al. 2004), which reveal higher chlorophyll concentrations in the fjords modulated by the high precipitation and river discharge that transports nutrients to the study area (Dávila et al. 2002). As for nutrients, their concentrations in the water column of the fjords' coastal zone are low due to high consumption by phytoplankton (Silva et al. 1997).

Information on microplankton composition in the Chilean fjords and adjacent areas is very scarce (Toro 1984, Avaria et al. 1997, Uribe 2001) limiting possible comparisons between water column vs. sediment species composition. However, in an attempt to make use of previous plankton data and compare the diatom composition in both environments (water column vs. sediments), it can be appreciated that the sediments are enriched in robust, highly silicified species (e.g., spores *Chaetoceros* spp., *Skeletonema costatum, Thalassionema nitzschioides*) and that these lack delicate species that are common in the plankton (e.g., *Asterionella formosa, Cylindrotheca closterium, Pseudo-nitzschia australis*). This difference suggests that there may have been an initial signal loss due to dissolution of delicate frustules during their descent through the water column and/or at the water-sediment interface. Albeit this loss, when comparing our results with the works of Toro (1984) and Uribe (2001), we can infer that the diatom assemblages preserved in the sediments of the Puyuhuapi Channel seem to reflect the most productive seasons in an annual cycle: spring (through the spores of *Chaetoceros)* and summer-autumn (with *Skeletonema costatum*, *Thalassionema nitzschioides* and *Rhizosolenia setigera/ pungens*), and that the river discharge signal is evidenced by the contribution of freshwater diatoms.

Freshwater diatoms in the Puyuhuapi Channel and their relationship with precipitation in the Chilean fjords

Temporal fluctuations in freshwater diatom abundance in marine coastal sediments

influenced by fluvial discharges have been widely used by various authors (e.g., Van Iperen et al. 1987, Pokras 1991, Uliana et al. 2001) to infer changes in river discharge and precipitation in the adjacent continent. A greater or lesser abundance of these organisms in coastal marine sediments would be related with humidity or aridity of the hinterland, respectively.

It is interesting to note that the freshwater diatom contribution recorded in the Puyuhuapi Channel sediments shows a clear general decreasing trend over time since the early 1900s (Fig. 7), and a sharp drop in the last 10 years. This trend is very notorious in core 35 where the freshwater diatom contribution diminishes from 34 % in 1905 to ~10 % in 1998-2001.

In order to explore if there is a relationship between freshwater diatom abundance in the Puyuhuapi Channel sediments with the precipitation records of the adjacent continent, we collected available precipitation data for two sites located nearby the study area, Puerto Cisnes (1955-2002) and Puerto Aysén (1931-1999)[3]. We lumped both records together to avoid missing data gaps, and calculated the standardized anomalies of precipitation for the period 1931-2002 (Fig. 8A). Two contrasting periods are evident in the anomaly record: (a) 1931-1971, with a high variability and both negative and positive anomalies, and (b) 1977-2002, with the majority of the period characterized by negative anomalies. When the precipitation record is compared to the standardized anomalies of freshwater diatom contribution (considering both cores together, Fig. 8B), a coincidence between the records is observed, and a reduction in both precipitation and freshwater diatom contribution since the mid-1970s (Fig. 8A, 8B) is especially evident.

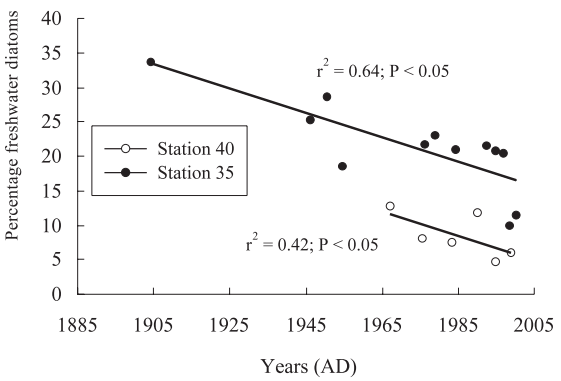

Fig. 7: Temporal variability in the percentage of freshwater diatoms during the last 100 years at stations 35 (black circles) and 40 (white circles). The linear regression equation with its r^2 and P values is indicated.

Variación temporal en el porcentaje de diatomeas de agua dulce durante los últimos 100 años en estaciones 35 (círculos negros) y 40 (círculos blancos). Se indica la ecuación de regresión lineal con su respectivo valor r^2 y P.

Furthermore, we also explored the relationship between these precipitation changes and global climatic changes related to the El Niño Southern Oscillation (ENSO). To this end, we plotted the Multivariate ENSO Index (MEI between the years 1950-2004), which is based on the observations of six variables: sea-level pressure, zonal and meridional components of the surface wind, sea surface temperature, surface air temperature, and total cloudiness fraction of the sky[3] (Fig. 8C). The MEI exhibits inter-annual and inter-decadal variability that, in general, characterizes the period 1950-1976 as a cold climatic period, followed by the interval 1977-1998 with numerous El Niño events and symbolizing a warm climatic period (e.g., Chávez et al. 2003). Comparing the three records in (Fig. 8), we can generalize that for the Puyuhuapi Channel area the cold period seems to be accompanied by greater precipitation and greater freshwater diatom contribution, while during the warm period the opposite occurred.

It is well-known that the inter-annual variability, especially in central Chile, is closely related to the ENSO cycle (Aceituno 1988, Karoly 1989). During an El Niño event, the weakening of the Pacific Anticyclone (PA) is accompanied by a northward displacement of the Southern Westerlies bringing heavy rainfall (and humid anomalies) to central Chile. In contrast, an expansion of the PA during La Niña events results in a southward movement (toward the pole) of these winds, reducing winter rainfall in the area. Quintana (2004) shows that the inter-decadal variability of precipitation in Chile has had an opposite

[3] See NOA (http://www.cdc.noaa.gov/ENSO/enso.mei_index.html)

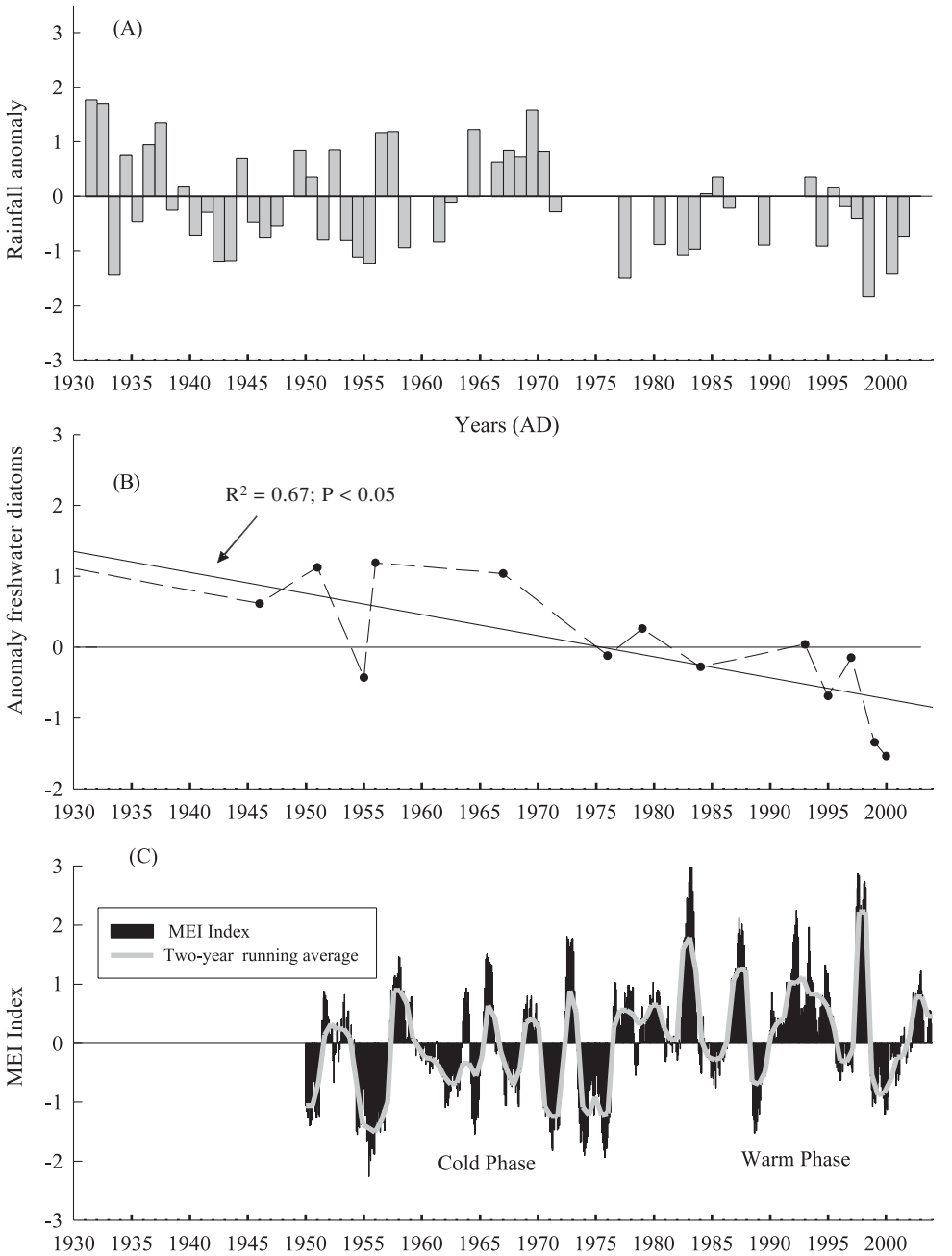

Fig. 8: (A) Record of the standardized rainfall anomaly for Puerto Cisnes and Puerto Aysén taken jointly (see text). (B) Freshwater diatom contribution at stations 35 and 40 (standardized anomaly and trend with its respective r^2 value). (C) Multivariate ENSO index (MEI) for the period 1950-2004. Positive values of the MEI represent the warm ENSO phase; negative values indicate the cold ENSO phase. In addition two long-term climatic periods are noted: one cold period between 1950 and 1976 followed by a warm period between 1977 and 1998. The gray line indicates the 2-year moving average.

(A) Registro de la anomalía estandarizada de la precipitación para Puerto Cisnes y Puerto Aysén tomados conjuntamente (ver texto). (B). Aporte de diatomeas de agua dulce en estaciones 35 y 40 (anomalía estandarizada y tendencia con su respectivo valor r^2). (C) Índice multivariado ENOS (MEI) para el período 1950-2004. Valores positivos del MEI representan la fase cálida del ciclo ENOS, los negativos indican la fase fría. Nótese que a su vez se distinguen dos grandes períodos climáticos, uno frío entre 1950-1976 seguido por uno cálido entre 1977-1998 y del 2002-2004. La línea gris indica la media móvil cada 2 años para el Índice MEI (1950-2004).

behavior between the southern and central regions over the last 100 years. Thus, we assume that the equatorward displacement of the Southern Westerlies during a warm phase of the ENSO cycle would diminish the precipitation in the study area, while the opposite would occur during the cold phase of ENSO.

In summary, the sedimentary evidence of an overall decrease in the contribution of freshwater diatoms since the 1970s would be closely related to a decrease in fluvial contribution and precipitation over the past ~ 30 years. Our observations agree with those of Quintana (2004) who states that the most significant reduction in precipitation in southern Chile (between 40-45º S) occurred in the last 30 years of the 20th Century. In addition, we could speculate that the reduced rainfall could be associated with the global oceanic and atmospheric warming of the past 20-30 years (Thompson & Solomon 2002, Karoly 2003).

CONCLUSIONS

The Puyuhuapi Channel, located at 44° S -70° W in the Chilean fjord system, is characterized by two distinct sedimentary environments. The head of the Channel, the Ventisquero Sound (station 35), registers the highest sedimentation rates accompanied by a greater accumulation of organic carbon, Si_{OPAL} and siliceous microorganisms, while the values of these parameters are lower in the middle part of the channel (station 40).

The sediments are characterized by a dominance of diatoms representative of high nutrient environments (e.g., spores of *Chaetoceros* spp.), accompanied by coastal planktonic (e.g., *Rhizosolenia setigera*/ *pungens*) and freshwater species. The latter reflects river discharges in the area. The silicoflagellate assemblage defines the Puyuhuapi Channel as a cold water environment.

A negative trend in the contribution of freshwater diatoms can be appreciated for the past ~30 years, suggesting that this could be associated with a drop in precipitation in the Chilean fjord area which, in turn, could be related to the global atmospheric and ocean warming of the last 20-30 years. In addition, we propose that freshwater diatom contribution is greater during cold (1950-1976) than during warm climatic periods (1977-1998).

ACKNOWLEDGEMENTS

The present research was financed by Grant 202.112.82-1 from the Research Office of the Universidad de Concepción awarded to Dr. C. Lange, by the CIMAR Fiordos-7 CPF 01-10 Project of the Comité Oceanográfico Nacional awarded to Dr. S. Pantoja, and by the FONDAP-COPAS Center. CONICYT financed the scholarship of L. Rebolledo. We appreciate comments and suggestions made by two anonymous referees, we also want to the thank Jeanne Simon for help with the English translation.

LITERATURE CITED

ACEITUNO P (1988) On the functioning of the Southern oscillation in the south American sector. Part I: Surface climate. Monthly Weather Review (USA) 116: 505-524.

ACHA EM, HW MIANZAN, RA GUERRERO, M FAVERO & J BAVÁ (2004) Marine fronts at the continental shelves of austral South America Physical and ecological processes. Journal of Marine Systems 44: 83-105.

AHUMADA R, A RUDOLPH & N SILVA (1996) Contenido de carbono total, carbono orgánico, carbono inorgánico, nitrógeno inorgánico y fósforo total, en los sedimentos de los fiordos de Campos de Hielo Sur. Ciencia y Tecnología del Mar (Chile) 19: 123-132.

ANDERSON DM & RB ARCHER (1999) Preliminary evidence of early deglaciation in Southern Chile. Palaeogeography, Palaeoclimatology, Palaeoecology 146: 295-301.

APPLEBY PG & F OLDFIELD (1978) The calculation of lead-210 dates assuming a constant rate supply of unsupported ^{210}Pb to the sediment. Catena 5: 1-8.

ARAYA JF (1997) Perfiles geomorfológicos de los fiordos y depresión longitudinal de norpatagonia. Ciencia y Tecnología del Mar (Chile) 20: 3-20.

ASTORECA R, G PIZARRO, MA PAREDES, P URIBE & V MONTECINO (2002) Relación entre patrones espaciales de productividad y la abundancia y estructura de tamaños del fitoplancton en sistemas de fiordos y canales de la XI Región. Comité oceanográfico nacional. Resultados preliminares del crucero CIMAR Fiordo 7: 77-88.

AVARIA S, D CASSIS, P MUÑOZ & P VERA (1997) Distribución del microplancton marino en aguas interiores del sur de Chile en octubre de 1995. Comité Oceanográfico Nacional 20: 107-123.

BINFORD M (1990) Calculation and uncertainty analysis of ^{210}Pb dates for PIRLA Project lake sediment cores. Journal of Paleolimnology (Canada) 3: 253-267.

BINFORD M & M BRENNER (1986) Dilution of ^{210}Pb by organic sedimentation in lakes of different trophic status, an application to studies of sediment-water interactions. Limnology and Oceanography 31: 584-595.

BORGEL R (1970) Geomorfología de las regiones australes de Chile. Revista Geológica de Chile 21: 135-140.

BROWER JE, JH ZAR & CN Von Ende (1998) Field and laboratory methods for general ecology. McGraw-Hill, Dubuque, Iowa, USA.194 pp.

CÁCERES M & A VALLE-LEVINSON (2004) Transverse variability of flow on both sides of a sill/contraction combination in a fjord-like inlet of southern Chile. Estuarine, Coastal and Shelf Science 60: 325-338.

CHÁVEZ F, J RYAN, S LLUCH-COTA & M ÑIQUEN (2003) From anchovies to sardines and back: Multidecadal change in the Pacific ocean. Science 299: 217-221.

COCHRAN JK, M FRIGNANI, M SALAMANCA, LG BELLUCI & S GUERZONI (1998) Lead-210 as a tracer of atmospheric input of heavy metals in the northern Venice Lagoon. Marine Chemistry 62: 15-29.

CUPP EE (1943) Marine plankton diatoms of the west coast of North America. Bulletin, Scripps Institution of Oceanography 5: 1-238.

DÁVILA P, D FIGUEROA & E MÜLLER (2002) Freshwater input into the coastal ocean and its relation with the salinity distribution off austral Chile (35°-55° S). Continental Shelf Research 22: 521-534.

DEVYNCK JL (1971) Perfil pluviométrico de Chile. Período: 1950-1969 y mapa pluviométrico: 1931-1960. Departamento de Geofísica, Universidad de Concepción, Concepción, Chile. 24 pp.

DGA (1987) Balance hídrico de Chile. Dirección General de Aguas, Ministerio de Obras Públicas, Chile. 24 pp.

FLYNN WW (1968) The determination of low levels of Polonium 210 in environmental materials. Analytical Chemical Acta 43: 221-227.

JENSEN KG & Ø MOESTRUP (1998) The genus *Chaetoceros* (Bacillariophyceae) in inner Danish coastal waters. Opera Botanica 133: 1-68 pp.

KAROLY DJ (1989) Southern Hemisphere circulation features associated with El Niño-Southern Oscillation events. Journal of Climatology 2: 1239-1252.

KAROLY DJ (2003) Ozone and climate change. Science 302: 236-237.

LAMY F, C RÜHLEMANN, D HEBBELN & G WEFER (2002) High- and low-latitude climate control on the position of the southern Peru-Chile Current during the Holocene. Paleoceanography 17: 1029-2001.

LEVITUS S & T BOYER (1994) World ocean atlas, Temperature NOAA Atlas NESDIS 4. Silver Spring, Washington District of Columbia, USA. Volume IV 117 pp.

MARGALEF R (1978) Diversity. In: Sournia (ed) Monographs on oceanographic methodology 6, phytoplankton manual, UNESCO, París, France. 370 pp.

MCCAFFREY R & JA THOMSON (1980) Record of the accumulation of sediment and trace metals in the Connecticut salt marsh. Advances in Geophysics 22: 165-236.

MORTLOCK RA & PN FROELICH (1989) A simple method for the rapid determination of biogenic opal in pelagic marine sediments. Deep-Sea Research 36: 1415-1426.

PANTOJA S, K HUGHEN, F GONZÁLEZ, J SEPÚLVEDA, C LANGE, P ROSSEL, G LORCA, P MUÑOZ, M SALAMANCA & A ÁVILA (2002) Registros de alta resolución de cambios climáticos y diagénesis en sedimentos de rápida depositación de los fiordos chilenos. Comité Oceanográfico Nacional, Resultados crucero Cimar-Fiordos 7: 101-106.

POKRAS EM (1991) Sources areas and transport mechanisms for freshwater and brackish-water diatoms deposited in pelagic sediments of the Ecuatorial Atlantic. Quaternary Research 35: 144-156.

QUINTANA J (2004) Estudio de los factores que explican la variabilidad de la precipitación en Chile en escalas de tiempo interdecadal. Tesis de Magíster en Ciencias Atmosféricas, Santiago, Departamento de Geofísica, Universidad de Chile, Chile. 93 pp.

RIVERA P (1981) Beiträge zur Taxonomie und Verbreitung der Gattung *Thalassiosira* Cleve. Bibliotheca Pycologica 56: 1-220.

ROJAS NH (2002) Distribución de materia orgánica, carbono y nitrógeno y diagénesis temprana en sedimentos de la zona canales australes entre los golfos Corcovado y Elefantes, Chile. Tesis de Oceanógrafo, Universidad Católica de Valparaíso, Valparaíso, Chile. 67 pp.

ROMERO O & D HEBBELN (2003) Biogenic silica diatom thanatocoenosis in surface sediments below the Peru-Chile Current: controlling mechanisms and relationship with productivity of surface waters. Marine Micropaleontology 48: 71-90.

ROUND EE, RM CRAWFORD & RM MANN (eds) (1990) The diatoms: biology and morphology of the genera. Cambridge University Press, Cambridge, United Kingdom. 747 pp.

SALAMANCA M (1996) Geocronología de los sedimentos. Comité Oceanográfico Nacional, Resultados Crucero Cimar-Fiordos 1: 64-68.

SCHRADER H & S GERSONDE (1978) Diatoms and silicoflagellates. In: WJ, Zachariasse et al. (eds) Micropaleontological counting methods and techniques-an exercise on an eight meter section of the Lower Pliocene of Capo Rosello, Sicily. Micropaleontology Bulletin Utrecht 17: 129-176.

SEPÚLVEDA J, S PANTOJA, K HUGHEN, C LANGE, F GONZÁLEZ, P MUÑOZ, L REBOLLEDO, R CASTRO, S CONTRERAS, A ÁVILA, P ROSSEL, G LORCA, M SALAMANCA & N SILVA (in press) Fluctuations in export productivity over the last century from sediments of a southern Chilean fjord (44 °S). Estuarine Coastal and Shelf Science.

SILVA N & S NESHYBA (1979) On the southernmost extension of the Perú-Chile undercurrent. Deep-Sea Research 26A: 1378-1393.

SILVA N & R PREGO (2002) Carbon and nitrogen spatial segregation and stoichiometry in the surface sediments of southern Chilean inlets (41-56°S). Estuarine, Coastal and Shelf Science 55: 763-775.

SILVA N, H SIEVERS & R PRADO (1995) Características oceanográficas y una proposición de circulación, para algunos canales australes de Chile entre 41º 20' y 46º 40' S. Revista de Biología Marina (Chile) 30: 207-254.

SILVA N, C CALVETE & H SIEVERS (1997) Características oceanográficas físicas y químicas de canales australes chilenos entre Puerto Montt y Laguna San Rafael (Crucero Cimar-Fiordo 1). Ciencia y Tecnología del Mar (Chile) 20: 23-106.

SILVA N, C CALVETE & H SIEVERS (1998a) Masas de agua y circulación general para algunos canales australes entre Puerto Montt y Laguna San Rafael, Chile (Crucero Cimar-Fiordo 1). Ciencia y Tecnología del Mar (Chile) 21: 17-48.

SILVA N, J MATURANA, J SEPÚLVEDA & R AHUMADA (1998b) Materia orgánica, C y N, su distribución y estequiometría, en sedimentos superficiales de la región norte de los fiordos y canales australes de Chile (Crucero Cimar-Fiordos 1). Ciencia y Tecnología del Mar (Chile) 21: 49-74.

SIMS PA ed (1996) An atlas of British diatoms. Biopress Ltd, Bristol United Kingdom. 601 pp.

TAKAHASHI K & P BLACKWELDER (1992) The spatial distribution of silicoflagellates in the region of the Gulf Stream warm-core ring 82B: applications to water mass tracer studies. Deep- Sea Research 39: 327-346.

THOMPSON DWJ & S SOLOMON (2002) Interpretation of recent southern hemisphere climate change. Science 296: 895-899.

TOMAS AC ed (1997) Identifying marine phytoplankton. Academic Press. San Diego, California,USA. 858 pp.

TORO J (1984) Determinación de las fluctuaciones mensuales de la abundancia y de la biomasa fitoplanctónica en el Estuario del Río Queule (Chile, IX Región). Revista de Biología Marina (Chile) 20: 23-37.

ULIANA E, CB LANGE & G WEFER (2001) Evidence for Congo River freshwater load in Late Quaternary sediments of ODP Site 1077 (5 S, 10 E). Palaeogeography, Palaeoclimatology, Palaeoecology 187: 137-150.

URIBE CP (2001) Diatomeas (Bacillariophyta) predominantes en la bahía de corral (Valdivia-Chile), Tesis de Magíster en Ciencias con mención en Botánica, Universidad de Concepción, Concepción, Chile, 138 pp.

VALLE-LEVINSON A, F JARA, C MOLINET & D SOTO (2001). Observations of intratidal variability of flows over a sill/contraction combination in a Chilean fiord. Journal of Geophysical Research 106: 7051-7064.

VAN IPEREN JM, TCE VAN WEERING, JHF JANSEN & AJ VAN BENNEKOM (1987) Diatoms in surface sediments of the Zaire deep-sea fan (SE Atlantic Ocean) and their relation to overlying water masses. Netherland Journal of Sea Research 21: 203-217.

WARREN C & M ANIYA (1999) The calving glaciers of southern south America. Global and Planetary Change 22: 59-77.

WITKOWSKI A, LANGE-BERTALOT H & D METZELTIN (2000) Diatom flora of marine coast I. Iconographia diatomologica annotated diatom micrographs. Vol. 7. Diversity-taxonomy-identification. Koeltzs Scientific Books, Königstein, Germany. 925 pp.

Associate Editor: Iván Gómez
Received July 28, 2004; accepted March 7, 2005

APPENDIX 1

Diatom ecological groups defined on the basis of their habitat according to Cupp (1943), Round et al. (1990), Sims (1996), Witkowski et al. (2000) and Romero & Hebbeln (2003)

Grupos ecológicos de diatomeas definidos en base a su hábitat, de acuerdo a información tomada de Cupp (1943), Round et al. (1990), Sims (1996), Witkowski et al. (2000) y Romero & Hebbeln (2003)

High nutrients (HN)

Resting spores *Chaetoceros* spp.
Chaetoceros cinctus Gran
Ch. constrictus Gran
Ch. coronatus Gran
Ch. debilis Cleve
Ch. diadema (Ehrenberg) Gran
Ch didymus Ehrenberg
Ch. radicans Shütt
Ch. vanheurcki Gran
Skeletonema costatum (Greville) Cleve
Thalassionema nitzschioides var. *nitzschioides* (Grunow) Grunow

Cold water (CW)

Thalassiosira gerloffii Rivera
T. pacifica Gran & Angst
Stellarima microtrias (Ehrenberg) Hasle & Sims
Rhizosolenia borealis Sundström

Warm water (WW)

Thalassiosira ferelineata Hasle & Fryxell
Odontella longicruris (Greville) Hoban
Chaetoceros lorenzianus Grunow

Coastal planktonic (CP)

Actinocyclus curvatulus Janisch
A. octonarius var. *sparsa* (Greg.) Hustedt
Actinocyclus sp.
Asteromphalus heptactis (Brébisson) Ralfs
Bacteriastrum sp.
Coscinodiscus radiatus Ehrenberg
C. marginatus Ehrenberg
C. perforatus Ehrenberg
Cyclotella litoralis Lange & Syvertsen
Ditylum brightwellii (West) Grunow
Lauderia annulata Cleve
Leptocylindrus minimus Gran (Hargraves)
Pseudo-nitzschia pungens (Grunow & Cleve) Hasle
Rhizosolenia setigera Brigthwell
R. pungens Cleve
Rhizosolenia sp.1
Stephanopyxis turris (Greville & Arnott) Ralfs
Thalassiosira aestivalis Gran & Angst
T. angulata (A. Schmidt) Hasle
T. anguste-lineata (A. Schmidt) G. Fryxell & Hasle
T. decipiens (Grunow) Jørgensen
T. delicatula (chilensis) Ostenfeld (in Bogert)
T. eccentrica (Ehrenberg) Cleve
T. mendiolana Hasle & Heimdal
T. oestrupii (Ostenfeld) Hasle
T. tenera Proschkina-Lavrenko
T. sp. 1
T. spp. (5-12µm)

Marine benthic (MB)

Actinoptychus senarius Ehrenberg (Ehrenberg)
A. vulgaris Schumann
Auliscus sp.
Cocconeis spp.
Dimeregramma minor (Gregory) Ralfs in Pritchard
Diploneis didyma (Ehrenberg) P.T Cleve
D. interrupta (Kützing) Cleve
Diploneis spp.
Grammatophora angulosa Ehrenberg
G. marina (Lyngbye) Kützing
*Hyalodiscus scoticus (*Kützing) Grunow
H. stelliger Bailey
Melosira arctica Dickie
M. nummuloides (Dillwyn) C.A Agarh
M. lineata (Dillwyn) Agardh
M. dickiei (Thwaites) Kützing
Opephora pacifica (Grunow) Petit
Paralia sulcata (Ehrenberg) Cleve
Plagiogramma interruptum (Gregory) Ralfs
Podosira sp.
Psammodictyon panduriforme (Gregory) Mann
Pseudohimantidium pacificum Hustedt & Krasske
Rhabdonema sp.
Stictodiscus californicus R.K. Greville
Surirella spp.

Freshwater (FW)

Achnanthes spp.
Amphora sp.
Aulacoseira granulata (Ehrenberg) Ehrenberg
Bacillaria paxillifer (O.F Müller) Hendey
Chaetoceros muelleri Lemmerman
Cyclotella ocellata Pantocsek
C. meneghiniana Kützing
C. stelligera (Cleve & Grunow) Van Heurck
Cyclotella spp.
Diatoma spp.
Ellerbeckia arenacea (Ralfs& More) Crawford
Eunotia sp.
Eunotograma laevis Grunow
Fragilaria construens var. *venter* (Ehrenberg) Grunow
Fragilaria sp.
Frustrulia sp.
Gomphonema constrictum Ehrenberg
Hantzschia amphioxys (Ehrenberg) Grunow
Hannaea arcus (Ehrenberg) Patrick
Mastogloia sp.
Melosira spp.
Navicula palpebralis Brébisson & Smith
Navicula sp.
Nitzschia frustulum H. Bennion
Nitzschia sp.
Pinnularia sp.
Rhoicosphenia curvata (Kützing) Grunow
Rhopalodia gibba (Ehrenberg) Müller
Rhopalodia sp.
Stauroneis phoenicenteron (Nitzsch) Ehrenberg
Synedra sp.
Tabularia tabulata (Kützing) (C.A Agardh) Snoeijs